

# Accretion disc outbursts: a new version of an old model

Jean-Marie Hamoury<sup>1</sup>, Kristen Menou<sup>2,3</sup>, Guillaume Dubus<sup>3</sup>, Jean-Pierre Lasota<sup>3</sup>  
and Jean-Marc Hure<sup>4</sup>

<sup>1</sup> UMR 7550 du CNRS, Observatoire de Strasbourg, 11 rue de l'Université, F-67000 Strasbourg, France

<sup>2</sup> Harvard-Smithsonian Center for Astrophysics, 60 Garden Street, Cambridge, MA 02138, USA

<sup>3</sup> UPR 176 du CNRS, Département d'Astrophysique Relativiste et de Cosmologie, Observatoire de Paris, Section de Meudon, F-92195 Meudon Cedex, France

<sup>4</sup> URA 173 du CNRS, Département d'Astrophysique Extragalactique et de Cosmologie, Observatoire de Paris, Section de Meudon, F-92195 Meudon Cedex, France

14 April 2024

## ABSTRACT

We have developed 1D time-dependent numerical models of accretion discs, using an adaptive grid technique and an implicit numerical scheme, in which the disc size is allowed to vary with time. The code fully resolves the cooling and heating fronts propagating in the disc. We show that models in which the radius of the outer edge of the disc is fixed produce incorrect results, from which probably incorrect conclusions about the viscosity law have been inferred. In particular we show that outside-in outbursts are possible when a standard binodal behaviour of the Shakura-Sunyaev viscosity parameter is used. We also discuss to what extent insufficient grid resolutions have limited the predictive power of previous models. We find that the global properties (magnitudes, etc. ...) of transient discs can be addressed by codes using a high, but reasonable, number of fixed grid points. However, the study of the detailed physical properties of the transition fronts generally requires resolutions which are out of reach of fixed grid codes. It appears that most time-dependent models of accretion discs published in the literature have been limited by resolution effects, in proper outer boundary conditions, or both.

**Key words:** accretion, accretion discs { instabilities { novae, cataclysmic variables { binaries : close

## 1 INTRODUCTION

The thermal-viscous accretion-disc instability model is more than 15 years old (see Cannizzo (1993b) for a historical overview). It is widely accepted that it provides the correct description of dwarf-nova outbursts and of ('soft') X-ray transient events. When, however, observations of these systems are compared with predictions of the model, the agreement is far from perfect (e.g. Lasota & Hamoury (1998) and references therein). It is sometimes also unclear what the predictions of the model are. One of the reasons for these uncertainties is the existence of various, different, versions of the model. From the very beginning these versions of the disc instability model differed in assumptions about viscosity and boundary conditions; they differed in the amount of matter accreted during the outburst, the shapes of light-curves, etc. (see Cannizzo (1993b)). At that time these differences seemed to be less important than the differences between the disc instability model and the competing, mass-transfer instability model (Bath & Pringle, 1981). The exponentially decaying tails of theoretical light curves predicted by the

mass-transfer model were thought to contradict observations (Cannizzo, 1993b) and the outer disc radius behaviour during and after outbursts seemed to favour the disc instability model (Ichikawa & Otsuki, 1992). The demise of the mass-transfer instability model was, however, caused by the lack of a physical mechanism which would trigger it.

With one model left it became important to establish just what its predictions are, and not merely whether it is better (or worse) than the competing model (Pringle, Verbunt & Wade 1986). The first systematic study of the disc instability model was presented by Cannizzo (1993a), who analysed the importance of various terms in the disc evolution equations and the influence of the numerical grid resolution on the outburst properties. Ludwig, Meyer-Hofmeister & Ritter (1994) studied general properties of disc outbursts, such as the location of the instability that triggers them. Recently Ludwig & Meyer (1998) analysed non-Keplerian effects which may arise during front propagation. The general conclusions of this group of studies were that non-Keplerian effects are negligible, that a few hundred grid points provide a sufficient resolution for the calculation results to be

independent of the number of grid points, and, finally, that with the usual assumption (see Smak (1984b) of a jump in the value of the viscosity parameter  $\eta$ , the model produces only 'inside-out' outbursts, i.e. outbursts starting in the inner disc regions. This last conclusion, if true, would entail changing the standard viscosity law (in which the parameter is constant in the hot and cool branch of the  $\eta$ - $T_e$  curve) because outbursts starting in the outer disc regions are clearly observed in classical dwarf-nova system SS Cyg (Mauche, 1996). This law already had to be modified when it was found (Smak, 1984b) that in order to get lightcurves similar to those observed in dwarf novae,  $\eta$  in outburst had to be larger than  $\eta$  in quiescence.

The absence of 'outside-in' outbursts in these studies, however, is just the result of keeping the outer disc radius constant in the calculations (Section 4.1) (Ichikawa & Osaki, 1992; Smak, 1984b); from this point of view, there is no reason to modify the viscosity prescription. This does not in itself prove that changes in viscosity are correctly described by the bimodal behaviour of the  $\eta$ -parameter (see e.g. Gammie & Menou 1998), but the reasons given for preferring other versions (the exponential decay from outburst being the principal one) are not compelling, and these versions involve more fundamental changes in the disc physics (see Lasota & Hamery 1998 for discussion and references).

For example, Cannizzo, Chen & Livio (1995) use the formula  $\eta = \eta_0 (H/R)^n$ , but to make the model work they have to 'switch off' convection. It is interesting, therefore, to recall that Faulkner, Lin & Pappalizou (1983) found dwarf nova outburst with  $\eta$  constant, but their model was criticized (Cannizzo, 1993b) because they claimed that convection has only a minor influence on the energy transport in the disc. These are not formal problems because the constant  $\eta$  models predict optically thin quiescent discs, whereas in bimodal models the quiescent disc is optically thick. There is observational evidence that dwarf nova discs in quiescence are optically thin (see Home, 1993 and references therein).

Conclusions about the number of grid points required to get resolution-invariant results seem, on inspection, too optimistic, especially because fronts are not resolved, a point which is particularly worrying for the heating fronts.

The present situation of the disc instability model seems to be confused. Various versions are based on different assumptions about the physical processes in the disc and numerical codes suffer either from incorrect boundary conditions or from insufficient resolution or from both. Quite often, in the case of explicit codes the resolution is limited by the required computer time.

In this article we describe a numerical model of time-dependent accretion discs, using an adaptive grid technique and an implicit numerical scheme, in which the disc size is allowed to vary with time. This numerical scheme allows rapid calculations of disc outburst cycles at very high resolution. These properties allow an easy comparison with other versions of the model and a systematic study of its various assumptions.

In the near future we will use our code to model various properties of dwarf novae and X-ray transients. The model was already used to model properties and outbursts of the dwarf nova W Z Sge (Lasota, Hamery & Hure, 1995; Hamery, Lasota & Hure, 1997) and the rise to outburst of the X-ray transient GRO J1655-40 (Hamery et al., 1997).

In §2 we discuss the time-dependent equations describing the disc radial structure and the implicit method used to solve them with a high spatial resolution. The vertical structure of the disc, and hence the heating and cooling terms that enter the time-dependent energy equation, are considered in §3. In §4 we present the results of our calculations and we discuss the importance of having sufficient numerical resolution and a correct boundary condition at the outer edge of the disc.

## 2 TIME-DEPENDENT ACCRETION DISCS

### 2.1 Disc equations

The basic equations for mass and angular momentum conservation in a geometrically thin accretion disc can be written as:

$$\frac{\partial \Sigma}{\partial t} = \frac{1}{r} \frac{\partial}{\partial r} (r v_r \Sigma) + \frac{1}{2r} \frac{\partial M_{\text{ext}}}{\partial r} \quad (1)$$

and

$$j \frac{\partial \Sigma}{\partial t} = \frac{1}{r} \frac{\partial}{\partial r} (r j v_r \Sigma) + \frac{1}{r} \frac{\partial}{\partial r} \left( \frac{3}{2} r^2 \Sigma \kappa \right) + \frac{j_k}{2r} \frac{\partial M_{\text{ext}}}{\partial r} - \frac{1}{2r} T_{\text{tid}}(r); \quad (2)$$

where  $\Sigma$  is the surface column density,  $M_{\text{ext}}(r)$  is the rate at which mass is incorporated into the disc at point  $r$ ,  $v_r$  the radial velocity in the disc,  $j = (GM_1 r)^{1/2}$  is the specific angular momentum of material at radius  $r$  in the disc,  $\kappa = (GM_1/r^3)^{1/2}$  is the Keplerian angular velocity ( $M_1$  being the mass of the accreting object),  $\eta$  is the kinematic viscosity coefficient, and  $j_k$  the specific angular momentum of the material transferred from the secondary.  $T_{\text{tid}}$  is the torque due to tidal forces, for which we use the value of Smak (1984b), derived from the determination of tidal torques by Pappalizou & Pingle (1977):

$$T_{\text{tid}} = c! r \frac{r^5}{a}; \quad (3)$$

where  $!$  is the angular velocity of the binary orbital motion,  $c$  is a numerical coefficient taken so as to give a stationary (or time averaged) disc radius equal to some chosen value, and  $a$  is the binary orbital separation.

Equation (2) is the standard form of angular momentum conservation, in which it is assumed that the azimuthal velocity  $v_\phi$  has the Keplerian value  $v_K$ . Ludwig & Meyer (1998) have considered deviations from Keplerian motion arising from strong pressure gradients (i.e. in the heating and cooling fronts) and found that these deviations only have a marginal influence on the outburst behaviour.

The energy conservation equation is taken as:

$$\frac{\partial T_c}{\partial t} = \frac{2(Q^+ - Q^- + J)}{C_p} - \frac{1}{C_p} \frac{\partial}{\partial r} (r v_r T_c) - v_r \frac{\partial T_c}{\partial r}; \quad (4)$$

where  $Q^+$  and  $Q^-$  are the surface heating and cooling rates respectively. They are usually taken as  $Q^+ = (9/8) \frac{\sigma_K}{K} T_e^4$  and  $Q^- = T_e^4$ ,  $T_e$  being the effective temperature (e.g. Cannizzo (1993a)). As described in §3 we use slightly different forms of these rates. The term  $J$  accounts for the radial energy flux carried either by viscous processes or by radiation. In the following, we neglect the radiative flux which,

according to Ludwig & Meyer (1998), is negligible, while according to Cannizzo (1993a) it is comparable to the viscous radial flux.

If viscosity is due to turbulence,  $J$  can be estimated in the framework of the parametrization. The flux carried in eddies with characteristic velocity  $v_e$  and size  $l_e$ , is:

$$F_e = C_P v_e \frac{\partial T_c}{\partial r} l_e = \frac{3}{2} C_P \frac{\partial T_c}{\partial r}; \quad (5)$$

in which case

$$J = 1 = r \frac{\partial}{\partial r} (r F_e); \quad (6)$$

A similar expression is obtained for radiative transport. Note that this expression differs slightly from that used by Cannizzo (1993a) which cannot be written as the divergence of a flux. Other prescriptions for  $J$  exist, in time-dependent simulations; they give results very similar to those obtained using Eq. (5).

## 2.2 Boundary conditions

So far there is no clear understanding of the physics of the interaction between the disc and the stream (see e.g. Armitage & Livio, 1997), and a fraction of the stream may spill over the disc. A proper treatment of the precise way in which matter is incorporated into the disc is far beyond our scope, and we use here the simplest, but very reasonable assumption that mass addition at the outer edge of the disc occurs in a very narrow region, so that the disc edge is very sharply defined. We can then write  $M_{\text{ext}}(r) = M_{\text{tr}}(r_0(t) - r)$  and  $\Sigma = \Sigma_0 Y(r_0(t) - r)$ , where  $M_{\text{tr}}$  is the mass transfer rate from the secondary star,  $Y$  is the Heaviside function,  $\delta$  is the Dirac function and  $\Sigma_0$ , the surface column density, is a smoothly varying function. The cancellation of the terms in the equation for mass and angular momentum conservation yields two boundary conditions, which can be written in the form:

$$M_{\text{tr}} = 2 r_0 \dot{r}_0 (\Sigma_0 - v_{r,0}) \quad (7)$$

and

$$M_{\text{tr}} \left( 1 - \frac{r_k}{r_0} \right)^{1=2} = 3 \dot{r}_0; \quad (8)$$

where the index 0 denotes quantities measured at the outer edge, and  $r_k$  is the circularization radius, i.e. the radius at which the Keplerian angular momentum is that of the matter lost by the secondary star, and  $\dot{r}_0$  is the time derivative of the outer disc radius. It is worth noting that the presence of a torque  $T_{\text{tid}}$  is required in this formulation, and it can be easily seen that no steady solutions exist when  $T_{\text{tid}} = 0$ .

Conditions (7, 8) take into account the fact that the outer edge of the disc can vary with time, and its position is controlled by the tidal torque  $T_{\text{tid}}$ . Variations of the disc radius are observed during outburst cycles in dwarf novae (Smak, 1984a; O'Donoghue, 1986; Wood et al., 1989; Wolf et al., 1993), with a rapid rise during the outburst and a decrease of the order of 20 percent during decline; such variations have been considered as a strong argument in favour of the disc instability model for dwarf novae, as opposed to the mass transfer instability model. The presence of 'superhumps' during SU UMa's superoutbursts is explained by the disc radius becoming larger than the radius for the

3:1 resonance (see e.g. Frank, King & Raine (1992)). O'saki (1996) assumes that the superoutbursts themselves are due to a 'tidal-thermal instability' which sets in when the disc's outer radius reaches the 3:1 resonance zone; see however Smak (1996).

Nevertheless it is often assumed, when modeling the normal outbursts, that the outer edge of the disc is fixed at a given radius, in which case Eq. (7) is used with  $\dot{r}_0 = 0$ , and Eq. (8) is replaced by  $r = r_0$ ; the tidal torque  $T_{\text{tid}}$  is also neglected in Eq. (2). This is equivalent to assuming that  $T_{\text{tid}}$  is negligible at  $r < r_0$  and becomes infinite at  $r = r_0$ . In view of the steep functional dependence of  $T_{\text{tid}}(r)$ , this might seem a reasonable approximation; however, we shall show that this is not the case at all, and that results obtained with both boundary conditions differ very significantly. An intermediate formulation has been proposed by Mineshige & O'saki (1985), who assume that the viscous stresses vanish at a fixed outer radius. This enables matter carrying angular momentum to leave the disc at its outer edge, at a rate which is comparable to the mass transfer rate.

We take, as usual,  $\Sigma = 0$  at the inner edge of the disc (more exactly, equal to a small value).

The thermal equation being a second order partial differential equation in  $r$ , two boundary conditions are required. However, except across a transition front between a hot and a cool region, the dominant terms in Eq. (4) are  $Q^+$  and  $Q^-$ . The highest order terms in the thermal equation are therefore negligible in almost all of the disc; the solutions of such equations are known to develop boundary layers, which adapt the internal solution (in which the highest order terms are neglected) to the boundary conditions. These boundary conditions are thus of no physical importance, and should be such as to minimize numerical difficulties. We have here taken  $\partial T_c / \partial r = 0$  at both edges of the disc.

## 2.3 Numerical method

We solve the set of equations (1, 2, 4) using a method described by Eggleton (1971). This method, which uses a variable mesh size, is a generalization of the Henyey method (Henyey et al., 1959), designed to solve the set of non-linear equations describing the internal structure of stars. The solutions of these equations have steep gradients, both at their surface and in the vicinity of the thin burning shells which appear after their evolution off the main sequence; moreover, the position of the shells is not fixed, but may vary relatively rapidly across the stellar envelope.

The natural abscissa,  $r$  in our case, is considered as an unknown variable of a new parameter  $q$  in the range  $0 \leq q \leq 1$  over the grid. The variable  $r$  varies according to:

$$\frac{dr}{dq} = W(r; T_c; \dots); \quad (9)$$

where  $W$  is a function which becomes small when the radial derivatives of  $T_c$  or become large, and is a normalization constant which adjusts the grid to the physical range covered by the variable  $r$ , so that

$$\frac{d}{dq} = 0; \quad (10)$$

Here, we take

$$W^2 = 1 + 0.05 \frac{(\partial \ln(r^{-1/2}))^2}{\partial \ln r} + 0.1 \frac{h \partial \ln T_c}{\partial \ln r} \quad (11)$$

The thermal and viscous equations (1, 2, 4) are equivalent to a set of four first order differential equations. These equations plus the two equations (9, 10) defining the grid are discretized and solved using a generalized Newton method. They can be written in the form:

$$\frac{dF_i(f^j)}{dq} = G_i(f^j); \quad (i = 1; l); \quad (12)$$

where  $l = 6$  is the number of equations, the  $f^j$  are the 6 variables  $r, \rho, T_c, \sigma, (\sigma^{-1/2}) = \sigma$  and  $\partial T_c = \partial r$ , and the  $G_i$  terms contain the time-derivatives. The discretized equation takes the form:

$$F_i(f_k^j) - F_i(f_{k-1}^j) - q [G_i(f_k^j) + (1 - \alpha_i)G_i(f_{k-1}^j)] = 0; \quad (13)$$

where  $q = 1/(N-1)$  is the mesh size,  $f_k^j$  is the value of the quantity  $f^j$  at the grid point  $k$  ( $k = 1; N$ ), and the  $\alpha_i$  are weights in the range  $[0; 1]$ . Values of  $\alpha_i$  equal to 0.5 lead to a second order scheme. The set of equations (13) is linearized (including Eq. (9-10) by numerical differentiation. This method has the advantage of being fully implicit, but convergence may be a problem when the initial guess is not close enough to the actual solution.

Whereas in Eggleton (1971) the time derivatives are expressed in their Eulerian form, we directly estimate the Lagrangean values by using either a linear or a cubic spline interpolation of the quantities calculated at the previous timestep, on the previous grid. The latter is more accurate, but requires a higher number of points when a transition front is present in the disc in order to avoid numerical oscillations.

This formulation does not guarantee that the disc mass is a conserved quantity within round-off errors. Instead, the disc mass has to be explicitly calculated by integrating over the disc extension, and deviations from mass conservation (easy to calculate given the inner and outer mass accretion rates in the disc, together with the time step of integration) provide valuable information on the quality of the code. We checked that all adaptive grid models presented here do indeed conserve mass accurately, except when we use too small a number of grid points (typically 100 or less). In the latter case, convergence is often a problem.

In order to improve the stability of the numerical scheme, we have used values of  $\alpha_i$  equal to 0 for the two equations defining the derivatives of  $T_c$  and  $\sigma$ , and to 1 for the two equations defining their second derivatives when the radius of the outer edge of the disc is kept fixed; we have also calculated the Lagrangean derivatives using linear interpolations. However, when  $r_0$  is allowed to vary, mass conservation is more difficult to enforce; we have taken all  $\alpha_i$  equal to 0.5 in that case, and used cubic splines to calculate the time derivatives. The timestep is chosen on empirical grounds and depends on the quality of the previous convergence. We end that initiating the disc with a hot steady solution or a globally cold state with an arbitrary profile gives, after a short transient period, equivalent results.

### 3 DETERMINATION OF THE EFFECTIVE TEMPERATURE

The vertical structure equations are very similar to those describing the internal structure of a star, with the notable exception that energy is dissipated everywhere in the vertical structure, including the optically thin regions, and that the vertical gravity comes from the central object.

In order to follow the time evolution of accretion discs, one needs to know the thermal balance ( $Q^+ - Q^-$ ) as a function of the central temperature  $T_c$  and the surface column density  $\Sigma$  at any radius in the disc. One should then be able to solve the full 2D energy transfer problem, which, in the thin disc approximation, is assumed to decouple into radial (Eq. (4)) and vertical equations. The latter, together with the reasonable assumption of vertical hydrostatic equilibrium, are as follows (Smak, 1984b):

$$\frac{dP}{dz} = -g_z = -\frac{2}{\kappa} \Sigma z; \quad (14)$$

$$\frac{d\Sigma}{dz} = 2; \quad (15)$$

$$\frac{d \ln T}{d \ln P} = r; \quad (16)$$

$$\frac{dF_z}{dz} = \frac{3}{2} \kappa P + \frac{dF_t}{dz}; \quad (17)$$

where  $P$ ,  $\rho$  and  $T$  are the pressure, density and temperature respectively,  $\Sigma$  is the surface column density between  $z$  and  $+z$ ,  $g_z = \frac{2}{\kappa} \Sigma z$  the vertical component of gravity,  $F_z$  the vertical energy flux and  $r$  the temperature gradient of the structure. This is generally radiative, with  $r = r_{\text{rad}}$ , given by:

$$r_{\text{rad}} = \frac{P F_z}{4P_{\text{rad}} \kappa g_z}; \quad (18)$$

$P_{\text{rad}}$  being the radiative pressure. When the radiative gradient is superadiabatic,  $r$  is convective ( $r = r_{\text{conv}}$ ). The convective gradient is calculated in the mixing length approximation, with a mixing length taken as  $H_{m1} = \alpha_m H_P$ , where  $H_P$  is the pressure scale height:

$$H_P = \frac{P}{g_z + (P/\rho)^{1/2} \kappa}; \quad (19)$$

which ensures that  $H_P$  is smaller than the vertical scale height of the disc. We have (Paczynski, 1969):

$$r_{\text{conv}} = r_{\text{ad}} + (r_{\text{rad}} - r_{\text{ad}})Y / (Y + A) \quad (20)$$

where  $r_{\text{ad}}$  is the adiabatic gradient, and  $Y$  is the solution of the cubic equation:

$$\frac{9}{4} \frac{2}{3 + \frac{2}{\alpha_m} Y^3 + V Y^2 + V^2 Y - V} = 0 \quad (21)$$

where  $\alpha_m = H_{m1}$  is the optical depth of the convective eddies. The coefficient  $V$  is given by:

$$V^2 = \frac{3 + \frac{2}{\alpha_m}}{3 \alpha_m} \frac{g_z^2 H_{m1}^2 C_P^2}{512 \rho^2 T^6 H_P} \frac{\partial \ln}{\partial \ln T_P} (r_{\text{rad}} - r_{\text{ad}}) \quad (22)$$

Here we take  $\alpha_m = 1.5$ , which is appropriate for solar type stars ( $\alpha_m$  ranges from 1 to 2 in solar models, see e.g. Guzik & Lebreton (1991) and Demarque and Guenther (1991)). One should note that  $\alpha_m = 1$  is generally used in the lit-

erature; as the disc vertical structure depends on the assumed  $\nu$  (Cannizzo, 1993b), we expect some difference from previous results.  $F_t$  is a time-dependent contribution that includes terms resulting from heating/cooling and contraction/expansion. This contribution is basically unknown, but it is most often assumed as proportional to  $P$ ; if this is the case, then Eq. (17) can be replaced by:

$$\frac{dF_z}{dz} = \frac{3}{2} \epsilon_{\text{eff}} \kappa P; \quad (23)$$

where  $\epsilon_{\text{eff}}$  may be considered as some effective viscosity. This coefficient is not known a priori and is generally different from the true viscosity parameter; the difference  $\epsilon_{\text{eff}}$  measures the departure from thermal equilibrium. The vertical structure, and hence the disc effective temperature at any given point, can therefore be obtained assuming that the disc is in thermal equilibrium, but with some unspecified  $\epsilon_{\text{eff}}$  different from  $\epsilon$ .

Even though this approximation is not unreasonable, and can be shown to be valid in the simplest case, that of a perfect gas and homologous cooling and contraction (Smak, 1984b), it is by no means justified and constitutes a significant drawback to the model. Other approximations have been used in the past; it is for example possible to assume that  $F_z$  has a given vertical profile; this is the approach of Mineshige & Osaki (1983) who assumed that  $F_z$  increases linearly with altitude up to a saturation value. This is not drastically different from assuming that  $F_t$  is proportional to pressure, since in both cases, energy is released in the densest regions of the disc, i.e. within one or a few scale heights from the mid plane. We have compared the results given in both cases, and we found that, for a given  $(\dot{M}; T_c)$ ,  $T_c$  being the central temperature, the effective temperatures obtained agreed to within 5 to 10%. Therefore, the cooling fluxes in time-dependent accretion discs are not determined better than to within 50%.

It would be highly desirable to have a better determination of  $Q$ ; however, this would require at least the introduction of explicitly time-dependent terms in the vertical structure equations, and that would couple the radial and vertical structure of the disc. This would enormously increase the required amount of computing time, making it very difficult to follow a complete outburst cycle with a reasonable number of radial grid points.

The viscous dissipation term  $3/2 \epsilon \kappa P$  in Eq. (17) is a direct consequence of the assumption that the radial-azimuthal component of the viscous stress tensor can be written  $\tau_r = \nu P$  (Shakura & Sunyaev, 1973). One should also note that the  $\nu$  prescription is used here in its local version, i.e. the local energy dissipation is assumed to be proportional to the pressure, which is by no means obvious.

Our approach is to determine  $Q$  for a number of values of  $T_c$ ,  $\dot{M}$ , and  $r$  and then perform a linear interpolation. In what follows, we have taken 70 equally logarithmically spaced values for  $r$  (190, 120 for  $T_c$ , respectively). This may seem time-consuming, but once the initial grid has been calculated, it is much more precise than the approach in which a sparse grid is used to construct analytic fits of  $Q$ . The "Te \ S-curves" are found numerically by looking in the grid for values of  $\dot{M}$ ,  $T_c$ , and  $r$  which satisfy the thermal equilibrium condition.

In thermal equilibrium the heating term  $Q^+$  is given by:

$$Q^+ = \frac{3}{2} \int_0^{Z_s} \kappa P dz; \quad (24)$$

which is close, but not exactly equal, to the heating term  $(9/8) \int_0^{Z_s} \kappa P dz$  generally used in the literature. Setting  $\epsilon_{\text{eff}} = 2/3 \epsilon_s = \epsilon_s / \kappa$ , and assuming that  $\epsilon_s$  is constant, one recovers the classical expression. This slight difference might appear as a minor inconsistency, but it may lead to unwanted numerical effects, since the equilibrium situation found when solving the radial structure would be different from that found in this section, and the disc may become unstable for a surface density slightly different from the expected critical value. For this reason, we prefer to use the exact value of the integral in (24) rather than its approximation; it is stored and interpolated in order to provide an accurate  $Q^+$  to the time-dependent runs.

We solved the vertical structure equations in two different approximations for the radiative transfer of energy, namely in the optically thick approximation and in the grey atmosphere approximation.

### 3.1 Optically thick case

The set of equations (14-16, 23) is integrated between the disc midplane and the photosphere, defined as the point where:

$$\tau_R P = \frac{2}{3} g_z; \quad (25)$$

where  $\tau_R$  is the Rosseland mean opacity.

The other boundary conditions are  $z = 0, F_z = 0, T = T_c, \kappa = 0$  at the disc midplane, and  $F_z = T^4, \kappa = \kappa_s$  at the photosphere.

### 3.2 Grey atmosphere approximation

For low values of the surface column density, the disc optical depth is no longer large. An accurate solution of the vertical disc structure would require an excessive amount of computing time, since frequency-dependent opacities would have to be taken into account for consistency. Instead, we chose to integrate the set of equations (14-15) down to optically thin regions, but we use a grey atmosphere approximation in which the temperature varies as  $T^4 = T_s^4 (1 + 3/4 \tau)$ , where  $T_s$  is the surface temperature and  $\tau$  the optical depth, given by:

$$\frac{d}{dz} = \tau; \quad (26)$$

For optical depths larger than unity, one should use Rosseland opacities  $\tau_R$ , whereas at small optical depths, the Planck mean opacities  $\tau_P$  are relevant. Here we take

$$\tau = \frac{\tau_R}{1 + \tau_R} + \frac{\tau_P}{1 + \tau_P}; \quad (27)$$

where  $\tau_R = \tau_R$  is the estimated disc optical depth. This  $T(\tau)$  relation leads to the following boundary condition at the surface:

$$F_z = 2 \int_0^{Z_s} T(\tau)^4 [E_2(\tau) + E_2(2\tau)] d\tau; \quad (28)$$

where  $E_2$  is the exponential-integral function. This relation can be approximated to better than 2% by

$$F_z = 2 T_s^4 (1 - e^{-2\tau_s} - 0.84 \tau_s^{-2} e^{-2\tau_s}); \quad (29)$$

where  $\tau_s$  is the optical depth from the midplane to the surface. The grey atmosphere approximation is rather crude (see e.g. Shaviv & Wehrse 1991; Hubeny 1990); moreover, it does not account for energy deposition in optically thin layers. However, calculations of the vertical disc structure using the Shaviv & Wehrse (1991) radiative transfer code show that the grey approximation is quite good, especially in view of uncertainties in  $Q$  mentioned above (Idan et al., 1998). In any case, the grey atmosphere approximation is required if one is willing to calculate a large number of such disc structures in a reasonable amount of computing time.

The two photospheric boundary conditions (25) and  $F_z = T_s^4$  are replaced by (29) and vanishingly small (we take here  $\tau_s = 10^{10} \text{ g cm}^{-2}$ ). The optical depth has to be explicitly integrated in the vertical structure. Consequently, Eq. (26) is added to the set of equations that we solve, with the associated boundary condition  $\tau_s = 0$  at the disc surface.

### 3.3 Numerical method

We solve the set of equations (14-17) for given values of the surface density  $\Sigma$  and central temperature  $T_c$  using the same adaptive grid numerical method as for the disc equations. The grid is now defined by:

$$W^2 = \frac{4}{z_{\text{nom}}^2} + \frac{1}{dz} \frac{d\kappa}{dz} + \frac{d \ln P}{dz} (1 + 2r^2); \quad (30)$$

where  $z_{\text{nom}} = (\kappa T_c)^{1/2}$  is the vertical scale height of the disc.

Because we have to solve the vertical structure for any given  $T_c$  and  $\Sigma$ ,  $\tau_s$  is not known a priori, but is a function of  $T_c$  and  $\Sigma$ . In other words, there is one more boundary condition than the number of differential equations, but one parameter is unknown. This can be formulated in a more classical problem by introducing a new equation:

$$\frac{d\tau_s}{dz} = 0; \quad (31)$$

We solve a set of 7 equations (14-17, 9, 10, 31) with 7 boundary conditions in the optically thick approximation, while Eq. (26) and the corresponding boundary condition are added to the problem in the grey atmosphere approximation. We take all weights  $w_i$  in Eq. (13) equal to 0.5.

### 3.4 Results

The equation of state of matter is interpolated from the tables of Fontaine et al. (1977); in the low temperature regime (below 2000 K), which is not covered by these tables, Saha equations are solved iteratively, as described by Paczynski (1969). The Rosseland mean opacities are taken from Cox & Tabor (1976) above 10,000 K, and from Alexander (1975) below. The Planck mean opacities are taken from Hure (1994), and cover the range 1000 - 30,000 K. The chemical composition is assumed to be solar. We note that Liu & Meyer-Hofmeister (1997) have shown that the use of improved (OPAL) opacities does not much affect the results of the vertical structure calculations, since most of the uncertainty resides in the prescription.

Figure 1 shows an example of the  $\{T_e\}$ -curves"

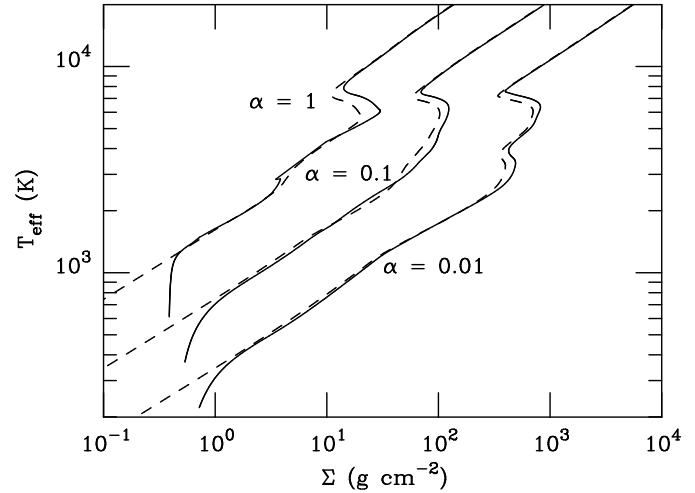


Figure 1.  $\{T_e\}$  curves for  $r = 10^{10} \text{ cm}$ ,  $M_1 = 1 M_\odot$ , and  $\alpha = 0.01, 0.1$  and  $1$ , in the grey atmosphere (solid line) and optically thick (dashed line) approximations.

we obtained, in both the optically thick and the grey atmosphere approximations. Differences are observed between the two cases, essentially when the disc is very optically thin (i.e. less than about  $1 \text{ g cm}^{-2}$ ), and when the disc is convective. The values  $\Sigma_{\text{max}}$  and  $\Sigma_{\text{min}}$  which define the upper and lower stable branches can be fitted, in the grey atmosphere approximation, by:

$$\Sigma_{\text{max}} = 13.1 \frac{M_1^{0.85}}{M} \frac{r}{10^{10} \text{ cm}}^{1.11} \text{ g cm}^{-2} \quad (32)$$

and

$$\Sigma_{\text{min}} = 10.4 \frac{M_1^{0.74}}{M} \frac{r}{10^{10} \text{ cm}}^{1.11} \text{ g cm}^{-2} \quad (33)$$

with the corresponding mass transfer rates:

$$\dot{M}_{\text{crit}}^- = 4.0 \cdot 10^{15} \frac{M_1^{0.04}}{M} \frac{r}{10^{10} \text{ cm}}^{2.67} \text{ g s}^{-1} \quad (34)$$

and

$$\dot{M}_{\text{crit}}^+ = 8.0 \cdot 10^{15} \frac{M_1^{0.03}}{M} \frac{r}{10^{10} \text{ cm}}^{2.67} \text{ g s}^{-1} \quad (35)$$

where  $\dot{M}_{\text{crit}}^-$  corresponds to  $\Sigma_{\text{max}}$  and  $\dot{M}_{\text{crit}}^+$  to  $\Sigma_{\text{min}}$ . We obtain in the optically thick case:

$$\Sigma_{\text{max}} = 13.4 \frac{M_1^{0.83}}{M} \frac{r}{10^{10} \text{ cm}}^{1.14} \text{ g cm}^{-2} \quad (36)$$

$$\Sigma_{\text{min}} = 8.3 \frac{M_1^{0.77}}{M} \frac{r}{10^{10} \text{ cm}}^{1.11} \text{ g cm}^{-2} \quad (37)$$

$$\dot{M}_{\text{crit}}^- = 4.0 \cdot 10^{15} \frac{M_1^{0.004}}{M} \frac{r}{10^{10} \text{ cm}}^{2.65} \text{ g s}^{-1} \quad (38)$$

$$\dot{M}_{\text{crit}}^+ = 9.5 \cdot 10^{15} \frac{M_1^{0.01}}{M} \frac{r}{10^{10} \text{ cm}}^{2.68} \text{ g s}^{-1} \quad (39)$$

These are in good agreement with values obtained previously (see e.g. Ludwig, et al. (1994)). A detailed comparison of our

$T_e$  curves with those obtained using the full radiative transfer equation is left for a future paper (Idan et al., 1998).

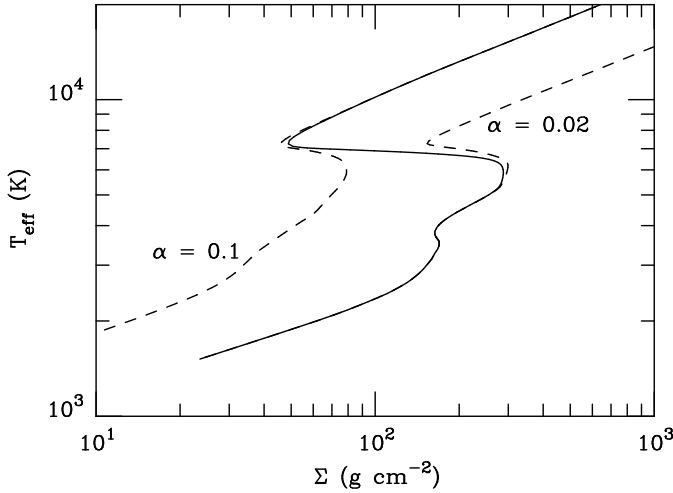


Figure 2. Modification of the  $T_{\text{eff}}$  curves when  $\alpha$  is no longer a constant. The dashed curves correspond to constant  $\alpha$ ,  $\alpha = \alpha_{\text{hot}}$  (left) and  $\alpha = \alpha_{\text{cold}}$  (right). The solid line is obtained for  $\alpha$  given by (40). The radius of interest is  $10^{10}$  cm, and the primary mass  $1.2 M_{\odot}$ .

#### 4 EVOLUTION OF DWARF NOVA DISCS

It is well known that models with constant values of  $\alpha$  cannot reproduce the observed light curves of dwarf novae (Smak, 1984b) (see however Faulkner et al., 1983). They predict that globally, the disc reaches neither the hot nor the cold branches. Instead a transition front propagates back and forth in a relatively narrow zone, producing rapid and small amplitude oscillations of the optical magnitude and the accretion rate. One can get around this difficulty if one assumes that  $\alpha$  is different on the hot and cold branch of the S-curves. In the following, we assume  $\alpha = \alpha_{\text{hot}}$  on the upper branch and  $\alpha = \alpha_{\text{cold}}$  on the lower branch, with the following temperature dependence for  $\alpha$ :

$$\log(\alpha) = \log(\alpha_{\text{cold}}) + \frac{[\log(\alpha_{\text{hot}}) - \log(\alpha_{\text{cold}})]}{1 + \frac{2.5 \cdot 10^4 \text{ K}}{T_c}} \quad (40)$$

The sharp transition between  $\alpha_{\text{cold}}$  and  $\alpha_{\text{hot}}$  is required if one wishes to keep the values of  $\dot{M}_{\text{in}}(\text{hot})$  and  $\dot{M}_{\text{in}}(\text{cold})$  in the effective S-curve equal to  $\dot{M}_{\text{in}}(\text{hot})$  and  $\dot{M}_{\text{in}}(\text{cold})$ .

Figure 2 shows the changes introduced in the  $T_{\text{eff}}$  curves when  $\alpha$  is given by Eq. (40).

Other prescriptions, that we do not consider here, have been proposed in the literature (Meyer & Meyer-Hofmeister, 1983; Cannizzo, Chen & Livio, 1995; Vishniac & Wheeler, 1996), such as  $\alpha = \alpha_0 (H=r)^n$  (see Lasota & Hamerly (1998) for a discussion of this prescription).

In what follows we use  $\alpha_{\text{cold}} = 0.01$  as it is commonly used in the literature. This assumption may be in contradiction with models of turbulent viscosity in accretion discs (Gammie & Menou, 1998).

In this article we only consider the case of dwarf novae in which the disc extends down to the white dwarf surface; its radius is taken from the Nauenberg (1972) mass-radius relation for white dwarfs. The visual ( $V$ ) magnitudes are computed assuming that each annulus of the disk emits

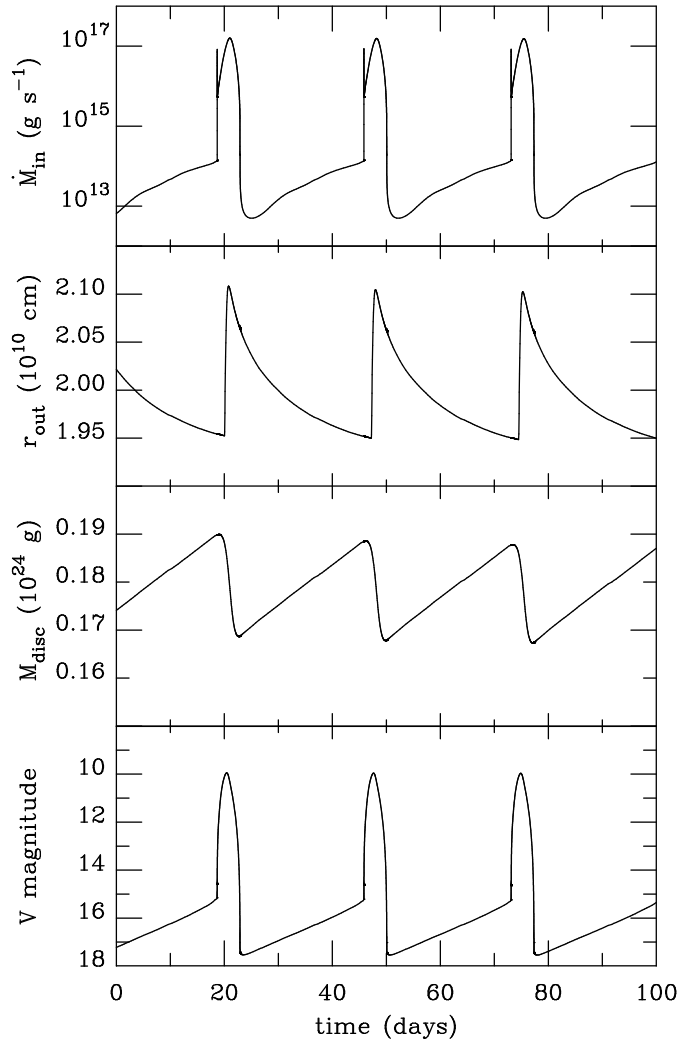


Figure 3. Outburst properties for  $M_1 = 0.6 M_{\odot}$ ,  $r_{\text{in}} = 8.5 \cdot 10^8$  cm,  $\alpha_{\text{cold}} = 0.04$ ,  $\alpha_{\text{hot}} = 0.20$ ,  $\langle r_{\text{out}} \rangle = 2 \cdot 10^{10}$  cm, and  $\dot{M}_{\text{in}} = 10^{16}$  g s $^{-1}$ . The upper panel shows the mass accretion rate onto the white dwarf, the second one the outer disc radius, the third one the disc mass, and the lower panel the visual magnitude.

blackbody radiation at the corresponding effective temperature.

Figures 3 and 4 show two models obtained for  $M_1 = 0.6 M_{\odot}$ ,  $r_{\text{in}} = 8.5 \cdot 10^8$  cm,  $\alpha_{\text{cold}} = 0.04$ ,  $\alpha_{\text{hot}} = 0.20$ , an average  $r_{\text{out}}$  of  $2 \cdot 10^{10}$  cm, and for mass transfer rates of  $10^{16}$  g s $^{-1}$  (Fig. 3) and  $10^{17}$  g s $^{-1}$  (Fig. 4). In the first case, the disc experiences inside-out outbursts, while in the second case, it experiences outside-in outbursts. The results concerning the evolution of the disc outer radius are in good agreement, at least from a qualitative point of view, with those previously obtained Ichikawa & Osaki (1992).

The typical surface density and central temperature radial profiles that we observe in our simulations are shown in Fig. 5. During the inward propagation of the cooling fronts, we recognize the density rarefaction wave that precedes the region of rapid cooling, while during the propagation of the heating fronts, we observe the density spike associated with the sharp region of rapid heating (Papalizou, Faulkner & Lin, 1983; Lin, Papalizou & Faulkner, 1985; Cannizzo,

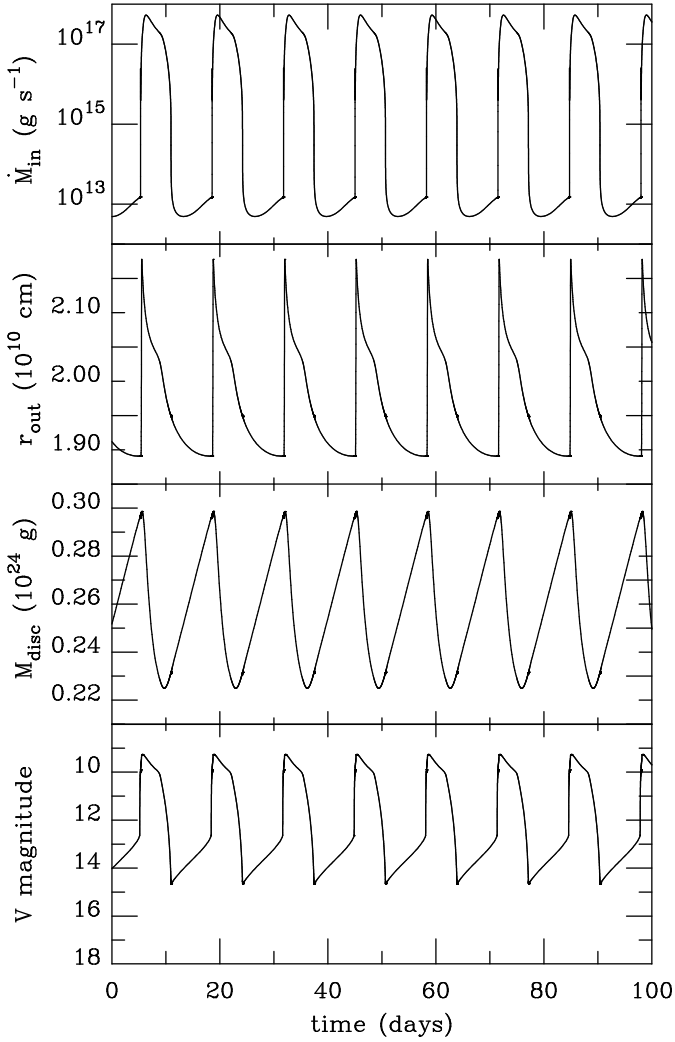


Figure 4. Same as Fig. 3, but for  $\dot{M} = 10^{17} \text{ g s}^{-1}$ .

1993a). We also note that our light curves are periodic (except when the number of points is so small that numerical errors are large).

#### 4.1 Effect of the outer boundary condition

We now take the same basic parameters as those used by Cannizzo (1993a) in his attempt to reproduce the light curve of SS Cyg. We take  $\tau_{\text{hot}} = 0.1$ ,  $\tau_{\text{cold}} = 0.02$ ; the mass transfer from the secondary is  $\dot{M}_T = 10^9 M_{\odot} \text{ yr}^{-1}$ , and the mass of the accreting white dwarf is  $M_1 = 1.2 M_{\odot}$  with an inner disc radius  $r_{\text{in}} = R_1 = 5 \times 10^8 \text{ cm}$ . We use the optically thick approximation for determining the cooling function  $Q$  of the disc. Our reference model uses 800 grid points.

It is worth noting that, because we do not use exactly the same cooling function (our values of  $\tau_{\text{in}}$  and  $\tau_{\text{ax}}$  differ by approximately 10 percent, and we do not use the same interpolation procedure between the cold and the hot branches of the S-curves, where  $\tau$  varies from  $\tau_{\text{cold}}$  to  $\tau_{\text{hot}}$ ), we do not expect to obtain quite the same result as Cannizzo (1993a); in particular, our model parameters have not been adjusted to fit SS Cyg's observed light curves.

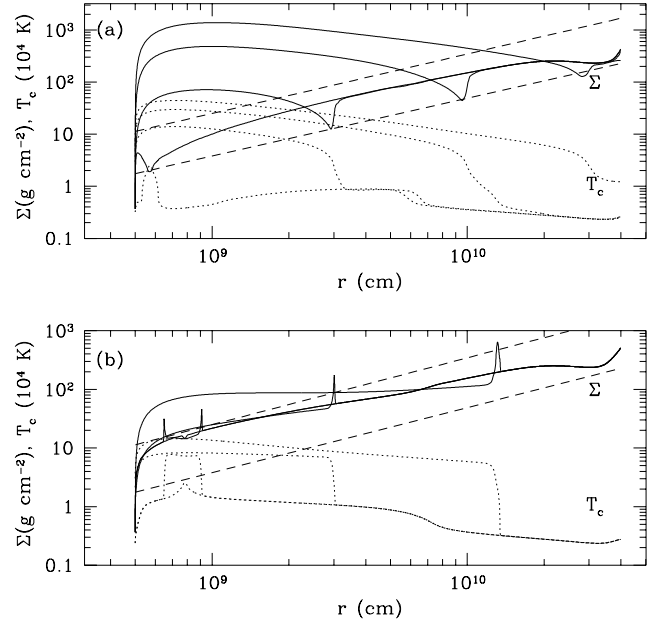


Figure 5. Typical profiles of the surface density (solid lines) and the central temperature  $T_c$  (dotted lines) observed during the evolution of the thin disc. (a) Inward propagation of a cooling front and the associated density rarefaction wave. (b) Outward propagation of an inside-out heating front and the associated density spike. The dashed lines represent  $\dot{m}_{\text{in}}$  (upper curve) and  $\dot{m}_{\text{ax}}$  (lower curve).

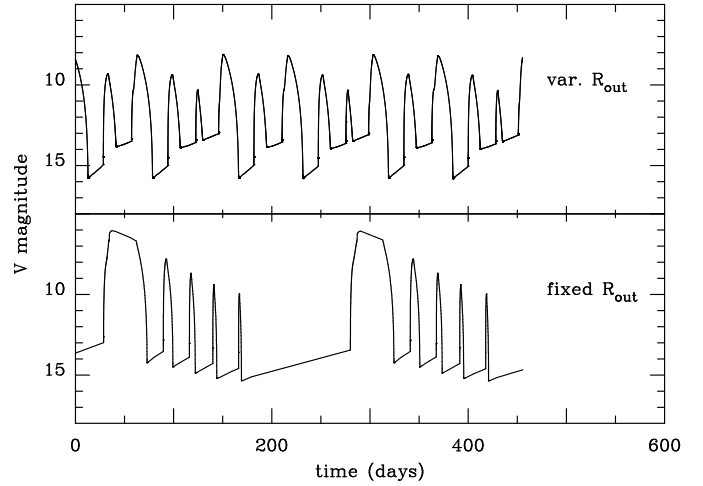


Figure 6. Calculated light curves assuming that the outer disc radius is fixed (lower panel), or that it may vary with time (upper panel). The average value of the outer disc radius is the same as in the fixed radius case.

Figure 6 shows the two light curves obtained when the outer disc radius is fixed at  $r_{\text{out}} = 4 \times 10^{10} \text{ cm}$ , and when  $r_{\text{out}}$  is allowed to vary, the constant  $c$  in Eq. (3) being such that the average value of  $r_{\text{out}}$  is also  $4 \times 10^{10} \text{ cm}$ .

In the first case, we do reproduce the results of Cannizzo (1993a) qualitatively: we have an alternative sequence of short and long outbursts, which are all of the inside-out type. There are some quantitative differences, which can be

attributed to the differences mentioned above, but the overall aspect is similar. In the second case, we obtain totally different results which, not surprisingly, are similar to those of Ichikawa & O saki (1992). We still obtain an alternating sequence of long and short outbursts, but both the number of short outbursts and the cycle length are quite different. As a rule, it is much easier to obtain such a sequence of alternating short and long outbursts when the outer radius is fixed than when it is allowed to vary.

When the outer edge of the disc is kept fixed at a constant value, we always observe inside-out outbursts, as did Cannizzo (1993a), Ludwig et al. (1994) and Ludwig & Meyer (1998). This is in contradiction with observations which show that, in a number of cases, the instability is triggered in the outer parts of the disc. Such a discrepancy has been attributed by Ludwig et al. (1994) to the fact that the disc might not extend to the white dwarf surface (note that this by itself would not suffice to give outside-in outbursts, since the instability would still be triggered in the innermost parts of the disc, but it could account for the UV delay). They also argued that the viscosity law could be more complex than the simple binodal prescription. However, when  $r_{\text{out}}$  is allowed to vary, we obtain outside-in outbursts for mass transfer rates high enough for the accumulation time of matter in the outer disc regions to be shorter than the viscous diffusion time.

The qualitative difference observed between the two cases is due to the fact that a much larger fraction of the disc is accreted during (large) outbursts when one assumes that  $r_{\text{out}}$  is constant: the density spike associated with the heating front brings some material to the outer edge of the disc, which splashes on the rigid wall implied by the boundary condition, and thus strongly increases  $\Sigma$ ; this matter will eventually be accreted until the cooling wave starts, when  $\dot{M} = \dot{M}_{\text{in}}$  at the outer edge of the disc; the accompanying rarefaction wave actually brings  $\Sigma$  below that value. The real situation is however quite different: when the density spike reaches the disc outer edge,  $r_{\text{out}}$  increases (matter carrying a large quantity of angular momentum flows outward), and the spike radially dies out. Thus the cooling wave starts earlier, at a stage where less mass from the outer disc has been accreted; moreover, during the quiescent phase, the disc contracts (the outward angular momentum flux is reduced), while mass transfer from the secondary continues. Both effects contribute to increase  $\dot{M}$  in the outer disc and help the occurrence of outside-in outbursts.

#### 4.2 Resolution Effects and the Disc Global Properties

The use of adaptive grids is an important improvement on previous time-dependent disc models in that the transition fronts are always resolved, whatever their location in the disc. This is illustrated in Fig. 7 where we show the sharpness of a heating front and contrast it with the actual width "seen" by the adaptive grid. A fair fraction of the grid (100 of the total 800 grid points in our reference model - adp800) is devoted to the front as a region of strong gradients. Note that the inner edge of the disc is also resolved by the grid.

We now evaluate the effect that degrading the numerical resolution has on the predicted light curves and on the variations of the total disc mass. We compare the relative

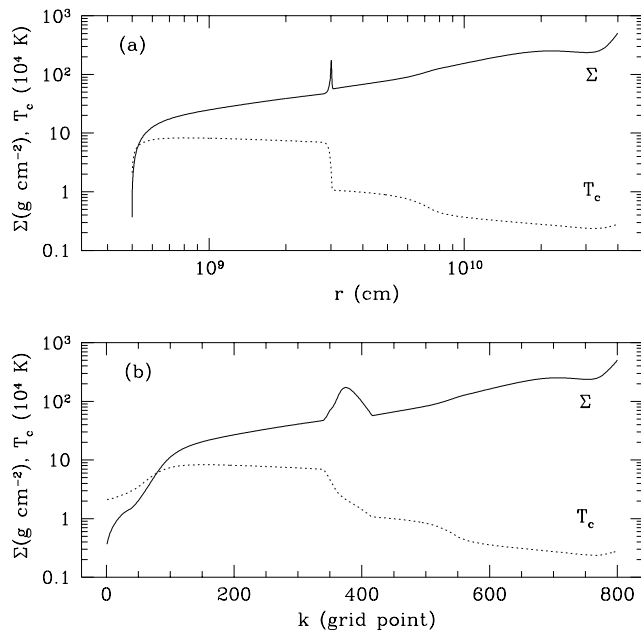


Figure 7. An example of the radial profiles of surface density (solid line) and central temperature  $T_c$  (dotted line) in the real space (a) and the grid space (b), using the adaptive grid at a resolution  $N = 800$  (reference model). The strong gradients are resolved by the grid and about 100 grid points are devoted to the resolution of the front itself.

merits of our code in an adaptive grid version and various fixed grid versions that we obtain when the grid function  $W$  in Eq. (9) is defined as a function of  $r$  only. In all cases, the outer radius has not been allowed to vary. We tested  $r$ ,  $\log$  and  $\text{sqr}$  grids (defined by a linear, a logarithmic and a square root spacing between grid points, respectively), but we concentrate here only on the results in the  $\text{sqr}$  grid case because this type of grid has been used extensively in the literature. Indeed, the viscous equation has a particularly simple form when the variables  $x = r^{-1/2}$  and  $S = x$  are used (Bath & Pringle, 1981). We report in Table 1 a few examples of grids and resolutions that have been used in time-dependent studies so far.

We investigate the fixed  $\text{sqr}$  and adaptive grids at resolutions  $N = 100; 400; 800; 1600$  and we refer to these models as adp100 to adp1600 and sqr100 to sqr1600. Figures 8 to 10 show the time evolution of the V magnitude and the total disc mass in these models. A straightforward conclusion is that a high numerical resolution ( $N \geq 400$ ) is required to reach a regime where the general shape of the outbursts becomes independent of the resolution. This is particularly true for the small outbursts, because the general aspect of the large ones is obtained at a relatively moderate resolution. The adaptive grid naturally requires a smaller number of grid points than the fixed grid to reach this regime (typically 200–400 points, compared with 800 points for the fixed grid). It is worth noting that most results in the literature have been obtained with resolutions which do not seem sufficient to avoid the resolution limits (see Table 1). The inadequacy of such a treatment is partially hidden by the fact that (1) the viscosity is a free parameter which can be deter-

Table 1. A sample of previous time-dependent studies of thin accretion discs, with the type of fixed grid and the numerical resolutions used. ‘System’ refers to a White Dwarf primary (WD, for the dwarf nova studies) and a black hole or neutron star primary (BH, for the black hole or neutron star Soft X-ray Transient studies). Note that Ichikawa & O saki (1992) and Sm ak (1994b) are the only studies in which the outer disc radius is allowed to move.

Study	System	Type of grid	Numerical Resolution
Sm ak (1984b)	WD	sqr	20–25
Lin, Papalbizou & Faulkner (1985)	WD	r/log	35
M ineshige (1987)	WD	log	401
M ineshige & W heeler (1989)	BH	log	21–41
Ichikawa & O saki (1992)	WD	r	35–45
Cannizzo (1993a)	WD	sqr	25–200
Cannizzo (1994)	BH/WD	sqr	300
Cannizzo, Chen & Livio (1995)	BH	sqr	103–1000
Cannizzo (1996)	WD	sqr	400
Cannizzo (1998)	BH	r/sqr/log	21–1000
Ludwig & Meyer (1998)	WD	?	200 (500)

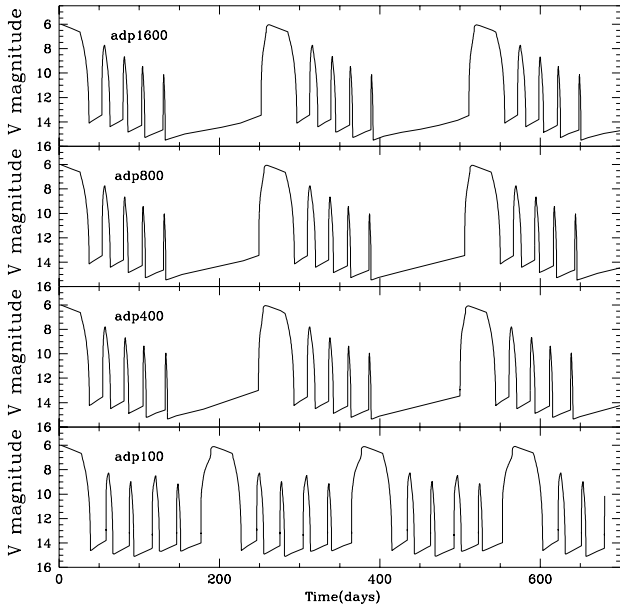


Figure 8. V magnitude light curves produced by our numerical model, using the adaptive grid at various resolutions: adp100 ( $N=100$ ), adp400 ( $N=400$ ), adp800 ( $N=800$ ), adp1600 ( $N=1600$ ). The outer radius is fixed at  $r_{\text{out}} = 4 \times 10^9$  cm.

mined only by confronting the time-dependent disc models with the observations, and (2) the cooling term  $Q$  that enters the thermal equation is not well known, and varies somewhat from one author to another. These two facts may account for two differences that we have with Cannizzo’s (1993a) results, even when we take his assumptions, parameters and number of grid points. Our small outbursts have peak amplitudes significantly smaller than the large outburst peak amplitudes. We also find that the evolution of the disc mass is almost independent on the resolution of the fixed sqr grid, in the sense that 50% of that mass is invariably accreted during large outbursts, whatever the resolution.

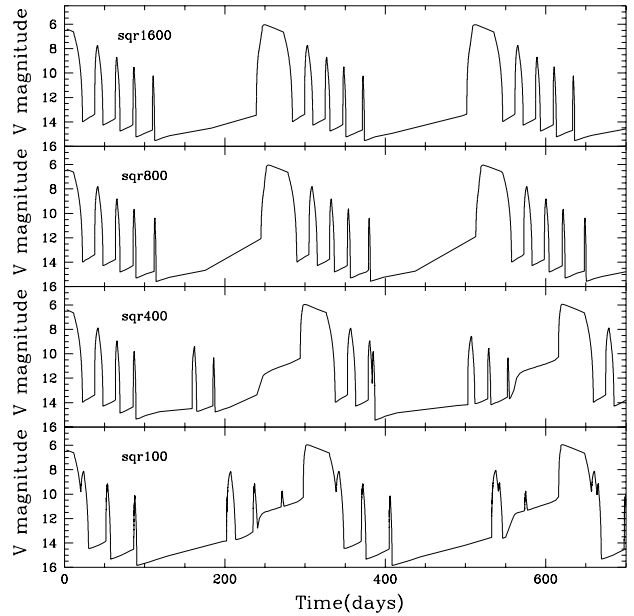


Figure 9. V magnitude light curves produced by our numerical model, using the fixed sqr grid at various resolutions: sqr100 ( $N=100$ ), sqr400 ( $N=400$ ), sqr800 ( $N=800$ ), sqr1600 ( $N=1600$ ).  $r_{\text{out}}$  is not allowed to vary.

#### 4.3 Resolution of the Transition Fronts

Until recently, numerical simulations were not able to resolve the structure of the transition fronts. For that reason, it has been very difficult to compare the predictions of semi-analytical models with the numerical results, and the physics of the fronts is not yet understood in much detail (Lin, Papalbizou & Faulkner, 1985; Cannizzo, 1994; Cannizzo, 1996; Cannizzo, Chen & Livio, 1995; Vishniac & Wheeler, 1996; Vishniac, 1997; Meyer, 1984; Meyer, 1986). We leave this comparison for a future paper, and here instead we determine the numerical resolution required to address this problem properly. A heating or cooling front which is not numerically resolved will be artificially enlarged; the physical

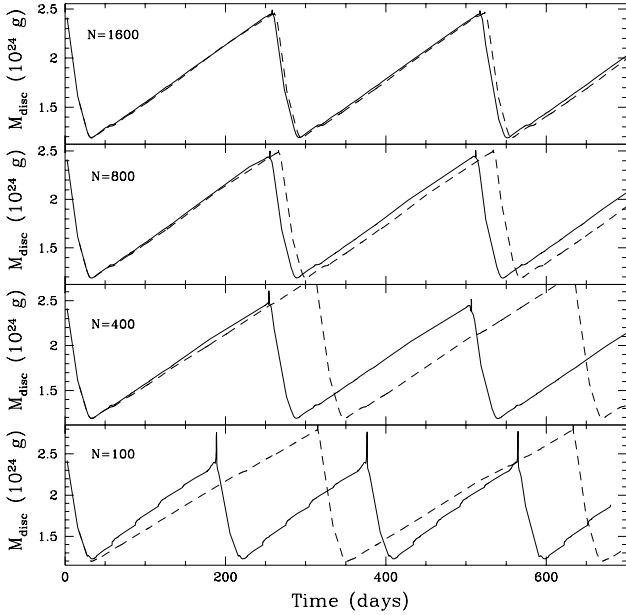


Figure 10. Evolution of the total disc mass with time for the various test models at numerical resolutions  $N = 100; 400; 800; 1600$ . The adaptive grid results are shown (solid lines) together with the fixed square grid results (dashed lines). In all cases,  $r_{\text{out}}$  is fixed.

results obtained in these conditions are very questionable. In the extreme case where a gradient (like a front) is limited to one numerical cell (between two grid points), the fluxes across the gradient are likely to be reduced and more of a numerical than a physical nature. Once again, one should keep in mind that uncertainties in the thermalequation (4), and in particular in the radial flux  $J_r$ , may well hide resolution effects. For instance, Cannizzo (1993a) shows that the light curves of dwarf novae do depend on the precise form of the thermalequation.

We show in Fig. 11 the fractional width,  $W = \Delta r$ , of the heating and cooling fronts during several outburst cycles of our test models. Note that  $W$  is the width over which 90% of the variation of  $\dot{M}$  (defined in Eq. (40)) occurs. This should not to be taken as a definitive value for the front width, but rather as a typical width (affected by resolution effects as well). What appears clearly in Fig. 11 is that fixed square grids do not resolve transition fronts well enough in the inner parts of the disc, even at high resolution. The discontinuities seen in the square model widths are signatures of the resolution limits and are very significant at low resolution ( $N = 100; 400$ ). The situation is systematically worse for heating fronts, which are sharper than cooling fronts. The adaptive grid has been devised to avoid large temperature and density differences between two grid points, and predicts the correct width for a moderate number of grid points  $N$ .

We also note that even when, close to the WD, the front widths are limited by the resolution, the resulting light curves may still be correct (square 800–1600). The basic reason is that the general outburst shape is not affected by what happens close to the compact object, where all characteristic timescales are small. On the other hand, an adaptive grid may approximately resolve the heating and cooling fronts,

but produce incorrect results at low resolution (for example when  $N = 100$ ). This is a result of too many grid points being used in steep gradient regions, which leaves too small a number of grid points in most parts of the disc.

#### 4.4 A Comparison of Numerical Grids

We define the fractional inter-grid spacing (hereafter FIS) between two grid points ( $k$  and  $k + 1$ ) as:

$$\frac{r}{r_{k+1} - r_k} = \frac{r_{k+1} - r_k}{(r_{k+1} + r_k)/2}; \quad (41)$$

where the index  $k$  refers to the grid point of interest in the grid extended from  $k = 1$  at the inner edge of the disc to  $k = N$  at the outer edge of the discs. A fixed square grid is defined by:

$$r_{k+1} = r_k + \Delta r; \quad (42)$$

being a constant depending on the resolution  $N$  used. In this case, the FIS is

$$\frac{r}{r_{k+1} - r_k} = \frac{r_N - r_1}{N} \frac{1}{r_k}; \quad (43)$$

A fixed square grid is defined by:

$$r_{k+1} = r_k + \Delta r; \quad (44)$$

and the corresponding FIS is

$$\frac{r}{r_{k+1} - r_k} = \frac{2 \left( \frac{r_N}{N} - \frac{r_1}{N} \right)}{N} \frac{1}{r_k}; \quad (45)$$

A log grid is defined by:

$$r_{k+1} = r_k \cdot \Delta r; \quad (46)$$

The corresponding FIS is

$$\frac{r}{r_{k+1} - r_k} = \frac{2 \left( \frac{1}{\Delta r} - 1 \right)}{1 + \Delta r}; \quad (47)$$

$$= \frac{r_N - r_1}{r_1} \frac{1}{N - 1}; \quad (48)$$

The adaptive grid runs show that the heating fronts reach a fractional width as low as  $W = \Delta r \approx 10^{-2}$ , and that  $W = \Delta r \approx 10^{-1.3}$  for the cooling fronts at the inner edge of the disc (see Fig. 11). This means that FISs of the order of  $(10^{-1.8}, 10^{-3.3}) / (10^{-2.5}, 10^{-4})$  are required if a grid is to resolve the cooling and heating fronts with 3/100 grid points respectively. We show in Fig. 12 the FISs for the square and log grids as a function of the numerical resolution  $N$ , and we compare them to the FISs required to resolve the cooling and heating fronts with 3 and 100 points. The comparison is performed at the inner edge of the disc ( $k = 1$ ) since fronts resolved there will be resolved everywhere in the disc: the front fractional widths increase with radius while the FISs of fixed grids are either constant (log grid) or decrease with radius (square and square grids).

The fixed grids require very high numerical resolutions to resolve in detail the fronts everywhere in the disc ( $N = 10^4 - 10^6$ ). The situation is worse when the accreting object is a black hole or a neutron star: the square and square grids will resolve the fronts less and less as the inner radius of the disc is reduced (see for example Cannizzo et al. (1995), Cannizzo (1998)). The log prescription has the advantage of defining a grid with a FIS which does not vary with radius.

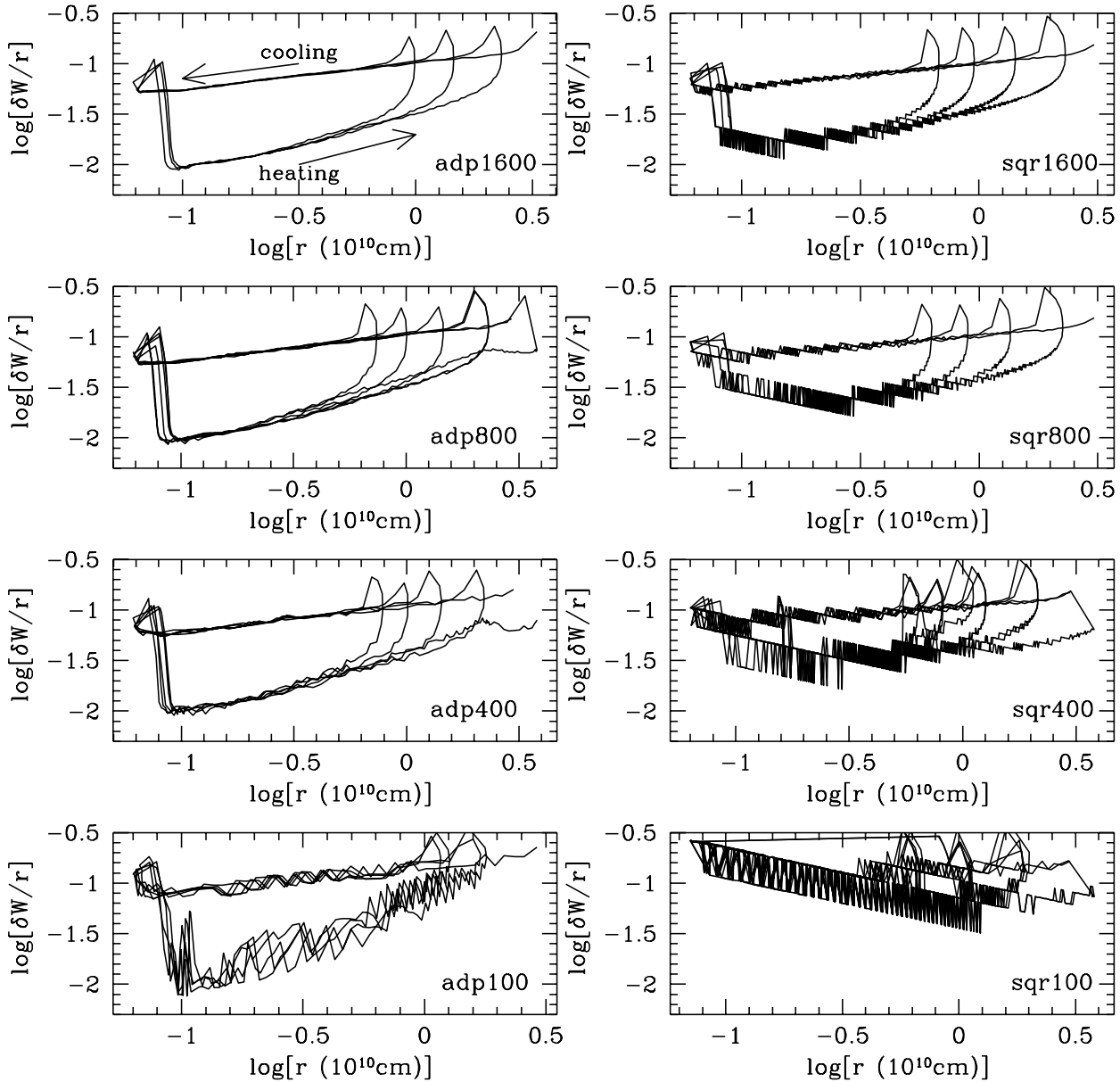


Figure 11. A comparison of the evolution with time of the cooling and heating front fractional widths ( $W/r$ ) as a function of the radius of location of the fronts in the disc for several outbursts. The left panel shows models with the adaptive grid at various resolutions, while the right panel shows models with the fixed sqg grid at the same resolutions. The inside-out heating fronts are sharper than the outside-in cooling fronts, which means that the evolution of the disc is anti-clockwise in these diagrams. The resolution effects are much more pronounced in the fixed sqg grid case than in the adaptive grid case and even at high resolution ( $N = 1600$ ), the fixed sqg grid does not resolve heating fronts better than marginally. At lower resolution, the results on the front widths are limited by resolution effects and are physically incorrect. At a resolution of  $N = 100$ , the front widths are clearly limited by the inter-grid spacing of the fixed sqg grid.

We conclude that reliable studies of the physical properties of transition fronts cannot be completed in a reasonable amount of computational time by fixed grid codes. An exception (see Fig. 11) is the structure of cooling fronts, which can probably be addressed, at least in the outer parts of the discs, by fixed sqg grid codes at high enough (but reasonable) numerical resolutions.

## 5 CONCLUSION

We have constructed a numerical code which can calculate, in a reasonable amount of computer time and at very high spatial resolutions, long cycles of accretion disc outbursts. This code works efficiently in the most general framework of the disc instability model and does not require special assumptions about viscosity or outer or inner radii. Its validity is of course limited by the way physical processes such

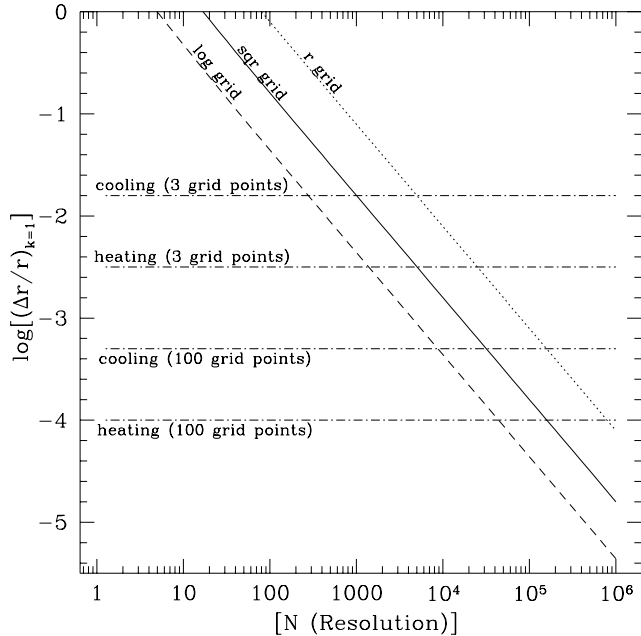


Figure 12. Dotted-dashed lines show the fractional inter-grid spacing ( $r=r$ , also FIS) required by various fixed grids in order to resolve the cooling and heating fronts of our reference model with 3 and 100 grid points at the inner edge of the disc ( $r_{in} = 5 \times 10^8$  cm), and consequently everywhere in the disc (see text). The comparison with the theoretical FIS of  $r$  (dotted line),  $\sqrt{r}$  (solid line) and  $\log$  (dashed line) grids, as a function of the numerical resolution  $N$ , illustrate the very high resolutions needed by fixed grids to resolve the transition fronts.

as turbulent viscosity, convection, radiative transfer etc. are treated. Of course it is also a 1D code modeling a fundamentally 2D (or even 3D) situation.

Since the mass of the central object enters the disc equations only in  $r_k$ , we expect most of our results to be valid for BH disc models as well (i.e. similar, but at a slightly smaller radius), as long as irradiation and general relativistic effects can be neglected.

In future work we intend to include effects of irradiation (Dubus et al. 1998) and to apply the code to a systematic study of dwarf nova outbursts and X-ray transient events.

Acknowledgments

We are grateful to J. Cannizzo, R. Narayan, F. Meyer, B. Popham, J. Raymond and J. Smak for useful discussions and to E. Quataert for comments on the manuscript. KM was supported by NASA grant NAG 5-2837.

REFERENCES

Alexander D.R., 1975, ApJS, 29, 363  
 Amittage P.J., Livio, M., 1997, ApJ in press, astro-ph/9709035  
 Bath G.T., Pingle J.E., 1981, MNRAS, 194, 967  
 Cannizzo J.K., 1993a, ApJ, 419, 318  
 Cannizzo J.K., 1993b, in Accretion Disks in Compact Stellar Systems, ed. J. Wheeler (Singapore: World Scientific), p. 6  
 Cannizzo J.K., 1994, ApJ, 435, 389

Cannizzo J.K., 1996, ApJ, 473, L41  
 Cannizzo J.K., 1998, ApJ, in press  
 Cannizzo J.K., Chen W., Livio M., 1995, ApJ, 454, 880  
 Cox A.N., Tabor J.E., 1976, ApJS, 31, 271  
 Demarque P., Guenther D.B., 1991, in Solar interior and atmosphere, eds. A.N. Cox, W.C. Livingston, M.S. Matthews, (Tucson: The University of Arizona Press), p. 1187  
 Dubus, G. et al., 1998, MNRAS, in preparation  
 Eggleton P.P., 1971, MNRAS, 151, 351  
 Faulkner J., Lind N.C., Papaloizou J., 1983, MNRAS, 205, 359  
 Fontaine G., Garaboske H.C. Jr., Van Horn H.M., 1977, ApJS, 35, 293  
 Frank J., King A.R., Raine D., 1992, in Accretion Power in Astrophysics, Cambridge University Press, Cambridge  
 Gamie C.F., Menou K., 1998, ApJ, 492, L75  
 Guzik J.A., Lebreton Y., 1991, in Solar interior and atmosphere, Cox A.N., Livingston W.C., Matthews M.S., eds, The University of Arizona Press, Tucson, p. 1235  
 Hamery J.-M., Lasota J.-P., Hure J.-M., 1997, MNRAS, 287, 937  
 Hamery J.-M., Lasota J.-P., McClinock J.E., Narayan, R., 1997, ApJ, 489, 234  
 Henyey L.G., Wilets L., Bohm K.H., LeVie R., Levee R.R., 1959, ApJ, 129, 628  
 Hubeny I., 1990, ApJ, 351, 632  
 Hure J.-M., 1994, PhD Thesis, Université Paris VII  
 Home K., 1983, in Accretion Disks in Compact Stellar Systems, ed. J. Wheeler (Singapore: World Scientific), p. 117  
 Ichikawa S., Otsuki Y., 1992, PASJ, 44, 15  
 Idan I., Hamery J.-M., Lasota J.-P., Shaviv G., 1998, MNRAS, in preparation  
 Lasota J.-P., Hamery J.-M., 1998, in Accretion Processes in Astrophysical Systems - Some Like it Hot, Proceedings of the 8th Annual October Conference in Maryland, AIP, in press  
 Lasota J.-P., Hamery J.-M., Hure J.-M., 1995, A & A, 302, L29  
 Lind N.L., Papaloizou J., Faulkner J., 1985, MNRAS, 212, 105  
 Liu, B.F., Meyer-Hofmeister, E., 1997, A & A, 328, 243  
 Ludwig K., Meyer F., 1998, A & A, 329, 559  
 Ludwig K., Meyer-Hofmeister E., Ritter H., 1994, A & A, 290, 473  
 Mache C.W., 1996, in Astrophysics in Extreme Ultraviolet, IAU Coll. 152, Bowyer S., Bowyer R.F., eds., Kluwer, Dordrecht, p. 317  
 Meyer F., 1984, A & A, 131, 303  
 Meyer F., 1986, MNRAS, 218, 7  
 Meyer F., Meyer-Hofmeister E., 1983, A & A, 128, 420  
 Mineshige S., 1987, Ap & SS, 130, 331  
 Mineshige S., Otsuki Y., 1983, PASJ, 35, 377  
 Mineshige S., Otsuki Y., 1985, PASJ, 37, 1  
 Mineshige S., Wheeler J.C., 1989, ApJ, 343, 241  
 Nauenberg M., 1972, ApJ, 175, 417  
 O'Donoghue D., 1986, MNRAS, 220, 23  
 Otsuki Y., 1996, PASP, 108, 39  
 Paczynski B., 1969, Acta Astronomica, 19, 1  
 Papaloizou J., Faulkner, J., Lind N.C., 1983, MNRAS, 205, 487  
 Papaloizou J., Pingle J.E., 1977, MNRAS, 181, 441  
 Pingle J.E., Verbunt F., Wade R.A., 1986, MNRAS, 221, 169  
 Shaviv G., Wehrhahn R., 1991, A & A, 251, 117  
 Shakura N.I., Sunyaev R.A., 1973, A & A, 24, 337  
 Smak J., 1984a, Acta Astr., 34, 93  
 Smak J., 1984b, Acta Astr., 34, 161  
 Smak J., 1996, in Cataclysmic Variables and Related Objects, IAU Coll. 158, Evans A., Wood J.H., Kluwer, Dordrecht, p. 45  
 Vishniac E.T., Wheeler J.C., 1996, ApJ, 471, 921  
 Vishniac E.T., 1997, ApJ, 482, 414  
 Wolsf., Mantel K.H., Barwig H., Schoenbsch R., Baumbantner O., 1993, A & A, 273, 160  
 Wood J.H., et al., 1989, MNRAS, 239, 809